Supplement of Geosci. Model Dev., 12, 2983–3000, 2019
https://doi.org/10.5194/gmd-12-2983-2019-supplement

*Supplement of*

# A simplified parameterization of isoprene-epoxydiol-derived secondary organic aerosol (IEPOX-SOA) for global chemistry and climate models: a case study with GEOS-Chem v11-02-rc

**Duseong S. Jo et al.**

*Correspondence to:* Jose L. Jimenez (jose.jimenez@colorado.edu)

## 1 IEPOX reactive uptake coefficient calculation

We use the resistor model equation by Gaston et al. (2014b) to calculate the reactive uptake coefficient of IEPOX (γ). The equation is as follows:

$$\frac{1}{\gamma} = \frac{\omega R_p}{4D_{gas}} + \frac{1}{\alpha} + \frac{\omega R_p}{4RTH_{org}D_{org}(q_{org}F - 1)} \tag{S1a}$$

$$\mathrm{F} = \frac{\coth\left(q_{org}\right) + h(q_{aq}, q_{org}^{*})}{1 + \coth\left(q_{org}\right) h(q_{aq}, q_{org}^{*})} \tag{S1b}$$

$$\mathrm{h}\left(q_{aq}, q_{org}^{*}\right) = -\tanh\left(q_{org}^{*}\right) \frac{\frac{H_{aq}D_{aq}}{H_{org}D_{org}}\left(q_{aq}\coth\left(q_{aq}\right) - 1\right) - \left(q_{org}^{*}\coth\left(q_{org}^{*}\right) - 1\right)}{\frac{H_{aq}D_{aq}}{H_{org}D_{org}}\left(q_{aq}\coth\left(q_{aq}\right) - 1\right) - \left(q_{org}^{*}\tanh\left(q_{org}^{*}\right) - 1\right)} \tag{S1c}$$

$$q_{org} = R_p\sqrt{\frac{k_{org}}{D_{org}}}, \quad q_{aq} = R_c\sqrt{\frac{k_{aq}}{D_{aq}}}, \quad q_{org}^{*} = \frac{R_c}{R_p}q_{org} \tag{S1d}$$

where $\omega$ is the mean molecular speed of IEPOX (m $s^{-1}$), $R_p$ is the particle radius (m), $D_{gas}$ is the gas-phase diffusion coefficient of IEPOX ($10^{-5}$ $m^2$ $s^{-1}$), α is the mass accommodation coefficient (0.1), $R$ is the universal gas constant (8.2057 x $10^{-2}$ L atm $mol^{-1}$ $K^{-1}$), T is temperature (K), $H_{aq}$ and $H_{org}$ are Henry's law coefficients in the aqueous core (1.7 x $10^7$ M $atm^{-1}$) and in the organic layer (2 x $10^6$ M $atm^{-1}$), $D_{aq}$ and $D_{org}$ are diffusion coefficients of IEPOX in the aqueous core ($10^{-9}$ $m^2$ $s^{-1}$) and in the organic layer (discussed below), and $R_c$ is the inorganic aqueous core radius (m). $k_{aq}$ is the first-order reaction rate constant in the aqueous phase ($s^{-1}$), calculated as follows:

$$k_{aq} = (k_{H^+}[H^+]) + (k_{nuc}[nuc]a_{H^+}) + k_{ga}[ga] \tag{S2}$$

where $k_{H^+}$ is the reaction rate constant due to acid-catalyzed ring-opening (0.036 $M^{-1}$ $s^{-1}$), [$H^+$] is the proton concentration (M), $a_{H^+}$ is the proton activity, $k_{nuc}$ is the reaction rate constant due to the presence of specific nucleophiles (sulfate and nitrate) (2 x $10^{-4}$ $M^{-1}$ $s^{-1}$), [nuc] is the concentration of nucleophiles (M), $k_{ga}$ is the reaction rate constant due to the presence of general acids (bisulfate) (7.3 x $10^{-4}$ $M^{-1}$ $s^{-1}$), and [ga] is the concentration of general acids (M). We assumed the reaction rate coefficient of IEPOX in the organic layer ($k_{org}$) is the same as $k_{aq}$. We note that the equation above is different from the IEPOX reactive uptake equation used by Zhang et al. (2018), which is based on Gaston et al. (2014a). The equation from Gaston et al. (2014a) can be derived from the Taylor series approximation by assuming thin coatings (Anttila et al., 2006). Therefore, we used the equation S1 to avoid some possible errors from the cases that second or higher order Taylor terms become important.

The diffusion coefficient of IEPOX in the organic layer ($D_{org}$) substantially changes by several orders of magnitude over a range of relative humidity (RH) in the atmosphere. Based on Table S3 of Zhang et al. (2018), we considered the RH dependence for $D_{org}$ values. Table S1 show $D_{org}$ values we used for GEOS-Chem calculation.

**Table S1**. Chemical reactions and dry deposition processes used in this study. The GEOS-Chem default chemistry mechanism is shown in the left column, and the corresponding lumped reactions used as the starting point of this work are shown in the right column.

| # | Reactions (GEOS-Chem v11-02-rc) | Reaction rate | Reactions (Lumped) | Reaction rate |
|---|---|---|---|---|
| 1 | ISOP + OH → 1.0 $ISOPO_2$ | 3.1E-11*exp(360/T) | ISOP + OH → 1.0 $ISOPO_2$ | 3.1E-11*exp(360/T) |
| 2 | ISOP + $O_3$ → other products | 1.00E-14*exp(-1970/T) | ISOP + $O_3$ → other products | 1.00E-14*exp(-1970/T) |
| 3 | ISOP + $NO_3$ → other products | 3.5E-12*exp(-450/T) | ISOP + $NO_3$ → other products | 3.5E-12*exp(-450/T) |
| 4 | ISOP + Cl → 1.0 $ISOPO_2$ | 7.60E-11*exp(500/T) | ISOP + Cl → 1.0 $ISOPO_2$ | 7.60E-11*exp(500/T) |
| 5 | $ISOPO_2$ + $HO_2$ → 0.628 ISOPOOH_A + 0.272 ISOPOOH_B + 0.037 ISOPOOH_D | 2.06E-13*exp(1300/T) | $ISOPO_2$ + $HO_2$ → 0.937 ISOPOOH | 2.06E-13*exp(1300/T) |
| 6 | $ISOPO_2$ + NO → 0.009 ISOPND + 0.081 ISOPNB | 2.7E-12*exp(350/T) | $ISOPO_2$ + NO → 0.009 ISOPND + 0.081 ISOPNB | 2.7E-12*exp(350/T) |
| 7 | $ISOPO_2$ + $CH_3O_2$ → other products | 8.37E-14 | $ISOPO_2$ + $CH_3O_2$ → other products | 8.37E-14 |
| 8 | $ISOPO_2$ + $ISOPO_2$ → other products | 2.30E-12 | $ISOPO_2$ + $ISOPO_2$ → other products | 2.30E-12 |
| 9 | $ISOPO_2$ + $CH_3CO_3$ → other products<br>$ISOPO_2$ + $CH_3CO_3$ → other products | 1.68E-12<br>1.87E-13 | $ISOPO_2$ + $CH_3CO_3$ → other products | 1.87E-12 |
| 10 | $ISOPO_2$ → other products | 4.07E+08*exp(-7694/T) | $ISOPO_2$ → other products | 4.07E+08*exp(-7694/T) |
| 11 | ISOPOOH_A + OH → 0.750 $ISOPO_2$<br>ISOPOOH_B + OH → 0.480 $ISOPO_2$<br>ISOPOOH_D + OH → 0.250 $ISOPO_2$ | 6.13E-12*exp(200/T)<br>4.14E-12*exp(200/T)<br>5.11E-12*exp(200/T) | ISOPOOH + OH → 0.652 $ISOPO_2$ | 5.69E-12*exp(200/T) |
| 12 | ISOPOOH_A + OH → 0.578 IEPOX_A<br>ISOPOOH_B + OH → 0.680 IEPOX_A + 0.320 IEPOX_B<br>ISOPOOH_D + OH → 0.500 IEPOX_D | 1.70E-11*exp(390/T)<br>2.97E-11*exp(390/T)<br>2.92E-11*exp(390/T) | ISOPOOH + OH → 0.697 IEPOX | 2.26E-11*exp(390/T) |
| 13 | ISOPND + OH → 0.1 IEPOX_D | 1.20E-11*exp(652/T) | ISOPND + OH → 0.1 IEPOX | 1.20E-11*exp(652/T) |
| 14 | ISOPNB + OH → 0.067 IEPOX_A + 0.033 IEPOX_B | 2.40E-12*exp(745/T) | ISOPNB + OH → 0.1 IEPOX | 2.40E-12*exp(745/T) |
| 15 | ISOPND + $O_3$ → other products | 2.90E-17 | ISOPND + $O_3$ → other products | 2.90E-17 |
| 16 | ISOPNB + $O_3$ → other products | 3.70E-19 | ISOPNB + $O_3$ → other products | 3.70E-19 |
| 17 | IEPOX_A + OH → other products<br>IEPOX_B + OH → other products | 3.73E-11*exp(-400/T)<br>5.79E-11*exp(-400/T) | IEPOX + OH → other products | 4.07e-11*exp(-400/T) |

|  |  |  |  |
|---|---|---|---|
|  | IEPOX_D + OH → other products | 3.20E-11*exp(-400/T) |  |
| 18 | IEPOX_A → IEPOX-SOA<br>IEPOX_B → IEPOX-SOA<br>IEPOX_D → IEPOX-SOA |  | IEPOX → IEPOX-SOA |
| 19 | ISOPND + hv → other products |  | ISOPND + hv → other products |
| 20 | ISOPNB + hv → other products |  | ISOPNB + hv → other products |
| 21 | ISOPOOH_A + hv → other products<br>ISOPOOH_B + hv → other products<br>ISOPOOH_D + hv → other products |  | ISOPOOH + hv → other products |
| 22 | ISOPOOH(A,B,D) dry deposition |  | ISOPOOH dry deposition |
| 23 | IEPOX(A,B,D) dry deposition |  | IEPOX dry deposition |

**Table S2**. Input parameter sets considered in this study for the evaluation of parameterizations using the box model.

| # | Species | Values |
|---|---|---|
| 1 | NO [ppt] | 1, 5, 10, 50, 100, 500, 1000, 5000, $10^4$, $5 \times 10^4$, $10^5$, $5 \times 10^5$, $10^6$ |
| 2 | OH [molecules $cm^{-3}$] | $10^4$, $5 \times 10^4$, $10^5$, $5 \times 10^5$, $10^6$, $2 \times 10^6$, $3 \times 10^6$, $4 \times 10^6$, $5 \times 10^6$ |
| 3 | $HO_2$ [ppt] | 1, 2, 5, 10, 20, 50, 100 |
| 4 | Aerosol pH [unitless] | -1,0,1,2,3,4 |
| 5 | Aerosol surface area [$um^2$ $cm^{-3}$] | 10, 50, 100, 500, 1000, 5000, $10^4$ |
| 6 | $O_3$ [ppb] | 10, 20, 30, 40, 50, 60, 70, 80, 90, 100 |
| 7 | $NO_3$ [ppt] | 1, 2, 5, 10, 20, 30 |
| 8 | Cl [molecules $cm^{-3}$] | 10, 100, 500, 1000, 5000 |
| 9 | $CH_3O_2$ [ppt] | 5, 10, 20, 30, 40, 50, 60, 70, 80, 90, 100 |
| 10 | $CH_3CO_3$ [ppt] | 0.5, 1, 2, 3, 4, 5, 6, 7, 8, 9, 10 |
| 11 | Aerosol radius [nm] | 50, 100, 150, 200, 250, 300, 500, 1000 |
| 12 | Organic coating fraction [unitless] | 0.0, 0.1, 0.2, 0.3, 0.4, 0.5, 0.6, 0.7, 0.8, 0.9 |
| 13 | Temperature [K] | 288, 293, 298, 303, 308, 313, 318 |
| 14 | Planetary boundary layer height [m] | 100, 200, 500, 1000, 1500, 2000, 2500, 3000, 3500, 4000 |
| 15 | Photolysis rate of ISOPOOH [$s^{-1}$] | $10^{-7}$, $5 \times 10^{-7}$, $10^{-6}$, $5 \times 10^{-6}$, $10^{-5}$, $2 \times 10^{-5}$ |

**Table S3**. Fitting constants for Eq. (12).

| Constant [Unit] | Value (PAR1) | Value (PAR3) |
|---|---|---|
| $C_0$ [s] | $1.2766\text{x}10^{6}$ | $8.6804\text{x}10^{5}$ |
| $C_1$ [s] | $-2.5853\text{x}10^{5}$ | $-6.8531\text{x}10^{5}$ |
| $C_2$ | 0.7812 | 0.8651 |
| $C_3$ [$s^{-1}$] | $1.1910\text{x}10^{-6}$ | $7.6927\text{x}10^{-7}$ |
| $C_4$ [s] | $-2.2937\text{x}10^{5}$ | $-1.8233\text{x}10^{5}$ |
| $C_5$ | 1.1969 | 0.91796 |
| $C_6$ [$s^{-1}$] | $3.2483\text{x}10^{-6}$ | $1.4389\text{x}10^{-6}$ |
| $C_7$ [s] | $-7.8766\text{x}10^{5}$ | $-1.8034\text{x}10^{5}$ |
| $C_8$ | 1.0760 | 1.3762 |
| $C_9$ [$s^{-1}$] | $1.5886\text{x}10^{-6}$ | $3.2078\text{x}10^{-6}$ |
| $C_{10}$ [s] | $-2.2735\text{x}10^{5}$ | |
| $C_{11}$ | 1.3584 | |
| $C_{12}$ [$s^{-1}$] | $3.3567\text{x}10^{-6}$ | |
| $C_{13}$ | -17.9610 | -9.084 |
| $C_{14}$ | 1.4992 | -2.004 |
| $C_{15}$ | $2.6901\text{x}10^{1}$ | $2.8313\text{x}10^{1}$ |
| $C_{16}$ | $1.8906\text{x}10^{1}$ | 9.9961 |
| $C_{17}$ | $4.5583\text{x}10^{-2}$ | $1.0903\text{x}10^{-1}$ |

**Table S4**. Computational time estimation using the Gprof performance analysis tool. Intel Fortran compiler 17.0.1 with '-p' option was used for the compilation process for function profiling. Values were based on 7-days simulation using 32 cores (2.3-GHz Intel Xeon E5-2697V4 processors) on the NCAR Cheyenne supercomputer. More than 1,000 subroutines in GEOS-Chem were analyzed with the Gprof but we classified subroutines to 12 categories by keywords. For example, if 'gckpp' was included in Fortran filename or subroutine name, it was considered as chemistry calculation process.

| Process | Estimated time [s] | Keywords for classification |
|---|---|---|
| Chemistry | 10728 | gckpp, flexchem, state_chm |
| Photolysis and non-tropospheric chemistry | 630 | strat_chem, fast_j |
| Emission | 1214 | hco |
| Transport | 2978 | transport, convection, tpcore |
| Dry deposition | 410 | drydep, mixing |
| Wet deposition | 4808 | wetscav |
| Unit conversion | 2146 | unitconv |
| VBS | 23 | soa, chem_nvoc, zeroin |
| PAR1 | 47 | par1$^{1)}$ |
| PAR2 | 13 | par2$^{1)}$ |
| PAR3 | 48 | par3$^{1)}$ |
| 3% | 1 | pari1$^{1)}$ |
| Others | 2732 | All others |

1) Not included in the standard version of GEOS-Chem

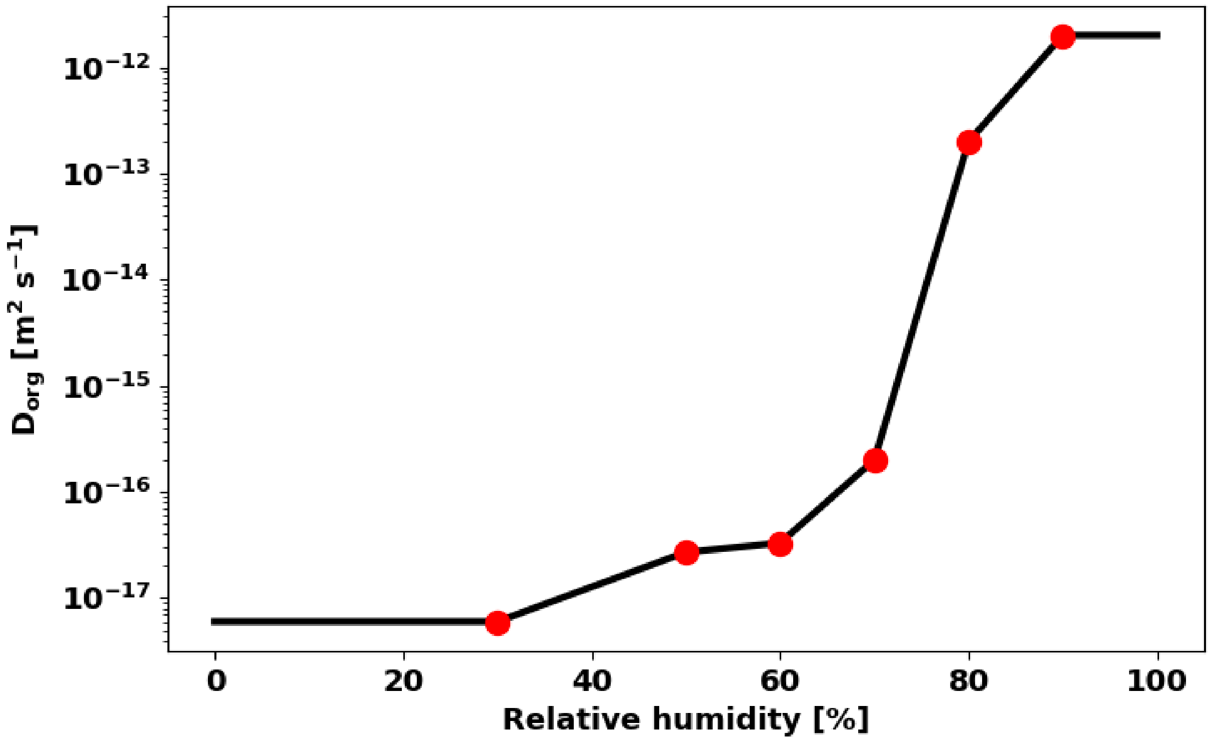

**Figure S1.** The diffusion coefficient of IEPOX in the organic layer ($D_{org}$) as a function of RH. Red points indicate values calculated by Zhang et al. (2018). Values in between red points are log-linearly interpolated, and values below 30% RH or above 90% are set to be the constant values.

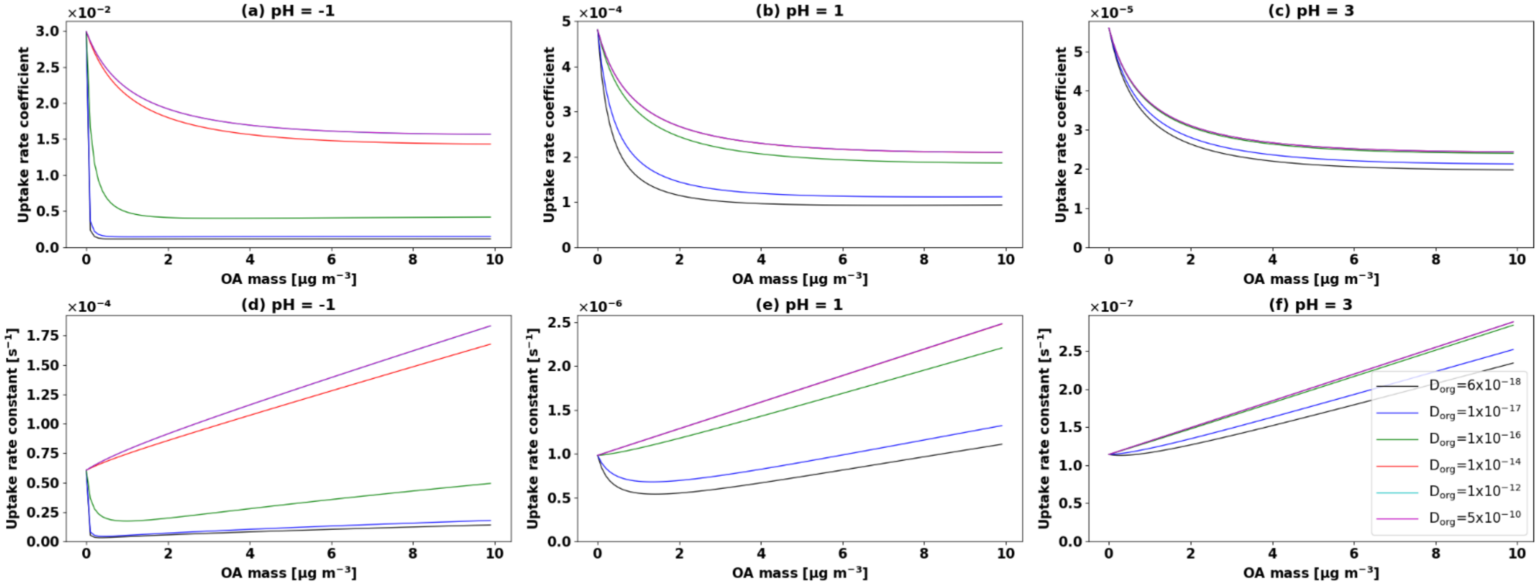

**Figure S2.** IEPOX reactive uptake coefficient (a,b,c) and uptake rate constant (d,e,f) as a function of OA mass concentrations. Different colors indicate $D_{org}$ values ranging from 6 x $10^{-18}$ to 1 x $10^{-12}$ $m^{-2}$ $s^{-1}$. Aerosol pH values were set to be -1 (a,d), 1 (b,e), and 3 (c,f), respectively. Sulfate aerosol mass concentration was assumed as 10 µg $m^{-3}$. Densities of sulfate and organic aerosols were set to be 1.7 and 1.3 g $cm^{-3}$, respectively, based on densities used by GEOS-Chem v11-02-rc. Initial aerosol radius of 50 nm and aerosol surface area of 3 x $10^{-6}$ $cm^2$ $cm^{-3}$ were assumed for organic aerosol mass = 0 µg $m^{-3}$. The changes of aerosol radius and aerosol surface area were calculated as OA mass increases, and aerosol inorganic core radius was fixed as 50 nm.

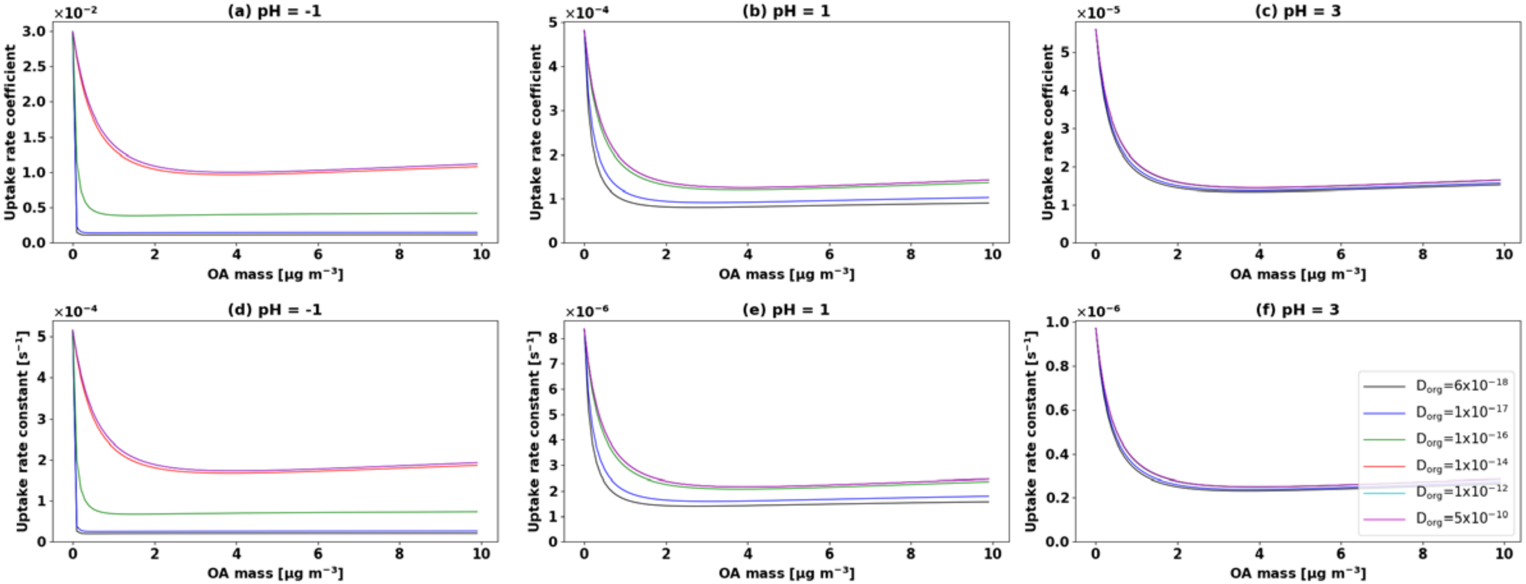

**Figure S3.** IEPOX reactive uptake coefficient (a,b,c) and uptake rate constant (d,e,f) as a function of OA mass concentrations. Different colors indicate $D_{org}$ values ranging from 6 x 10$^{-18}$ to 1 x 10$^{-12}$ m$^{-2}$ s$^{-1}$. Aerosol pH values were set to be -1 (a,d), 1 (b,e), and 3 (c,f), respectively. Sulfate aerosol mass concentration was assumed as 1 µg m$^{-3}$. Densities of sulfate and organic aerosols were set to be 1.7 and 1.3 g cm$^{-3}$, respectively, based on densities used by GEOS-Chem v11-02-rc. Initial aerosol radius of 50 nm and aerosol surface area of 3 x 10$^{-6}$ cm$^{2}$ cm$^{-3}$ were assumed for organic aerosol mass = 0 µg m$^{-3}$. The changes of aerosol radius and aerosol surface area were fixed regardless of OA mass increase. Aerosol core radius was reduced in proportion to the OA mass increase (i.e. coating thickness increase).

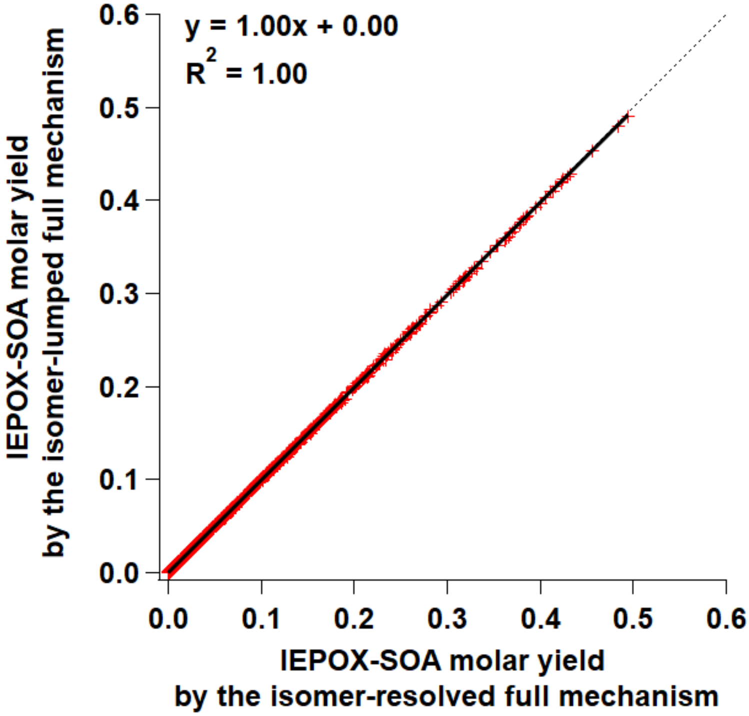

**Figure S4.** Point to point comparison of IEPOX-SOA molar yields for the isomer-lumped (y-axis) versus isomer-resolved full GEOS-Chem (x-axis) mechanisms. Yields were calculated by the box model using 14,000 simulations by systematically varying the input parameters in Table S2.

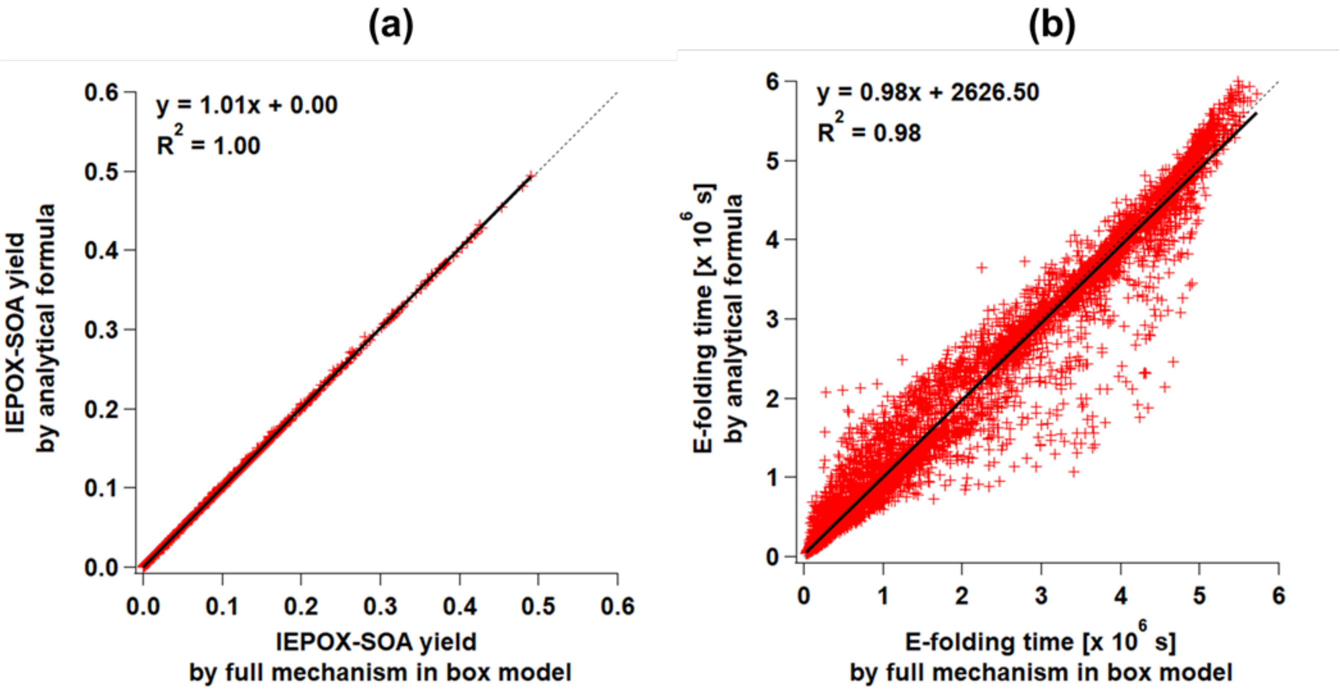

**Figure S5.** Scatterplots of parameterized (PAR1 case) (y-axis) versus simulated (x-axis) results by the box model for (a) IEPOX-SOA molar yield and (b) formation timescale with randomly selected parameters in Table S1 of 14,000 simulations.

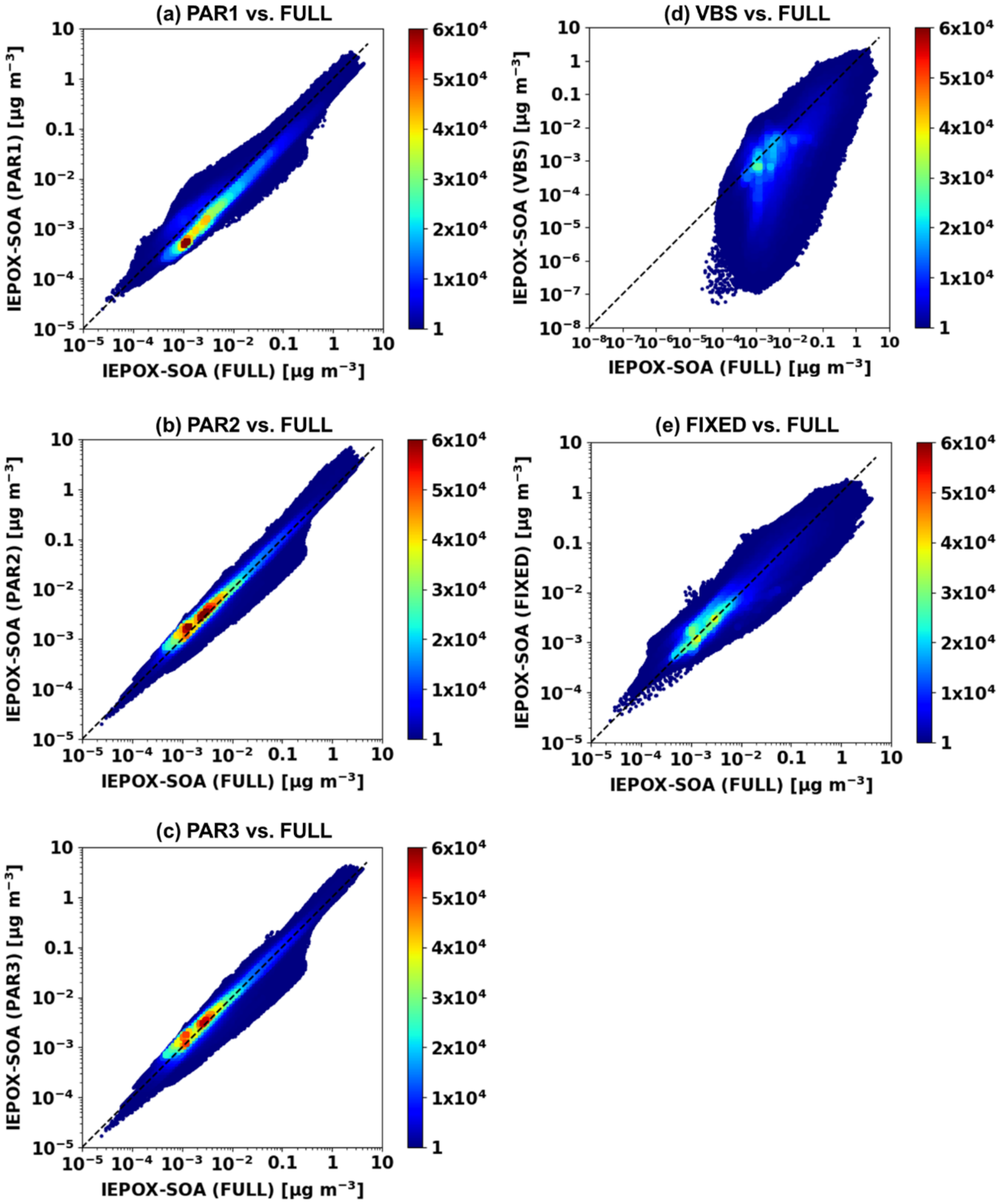

**Figure S6.** Scatterplots of parameterized (y-axis) versus full chemistry IEPOX-SOA (x-axis) concentrations within the troposphere for July 2013 – June 2014 shown on a log scale with base of 10. Each point represents monthly averaged model grid value of IEPOX-SOA concentration. Colors represent the density of points, where densities were calculated by dividing x and y axis ranges into 100 by 100 grid cells.

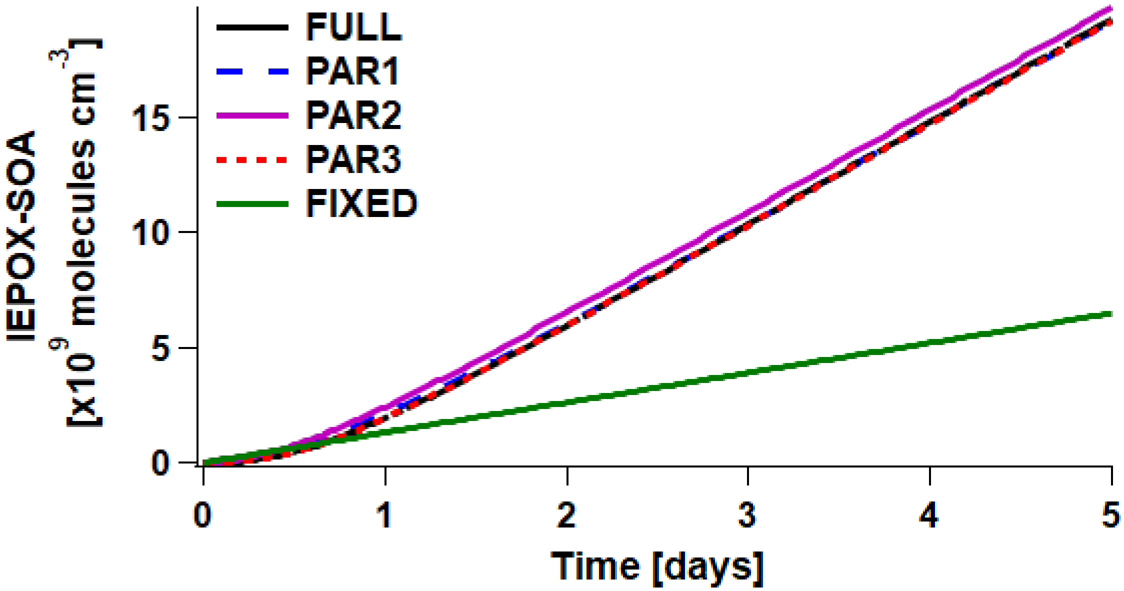

**Figure S7.** Same as Fig. 4d but IEPOX-SOA concentrations were simulated without diurnal variation of chemical/meteorological fields. Fixed values used for this calculation are: OH = $10^6$ molecules cm$^{-3}$, $HO_2$ = 100 ppt, $O_3$ = 50 ppb, $NO_3$ = 10 ppt, Cl = $10^3$ molecules cm$^{-3}$, NO = 100 ppt, $CH_3O_2$ = 10 ppt, $CH_3CO_3$ = 10 ppt, IEPOX uptake rate = $10^{-5}$ s$^{-1}$, Dry deposition rate of ISOPOOH and IEPOX = $10^{-6}$ s$^{-1}$, ISOPOOH photolysis rate = $10^{-5}$ s$^{-1}$, temperature = 298.15 K.

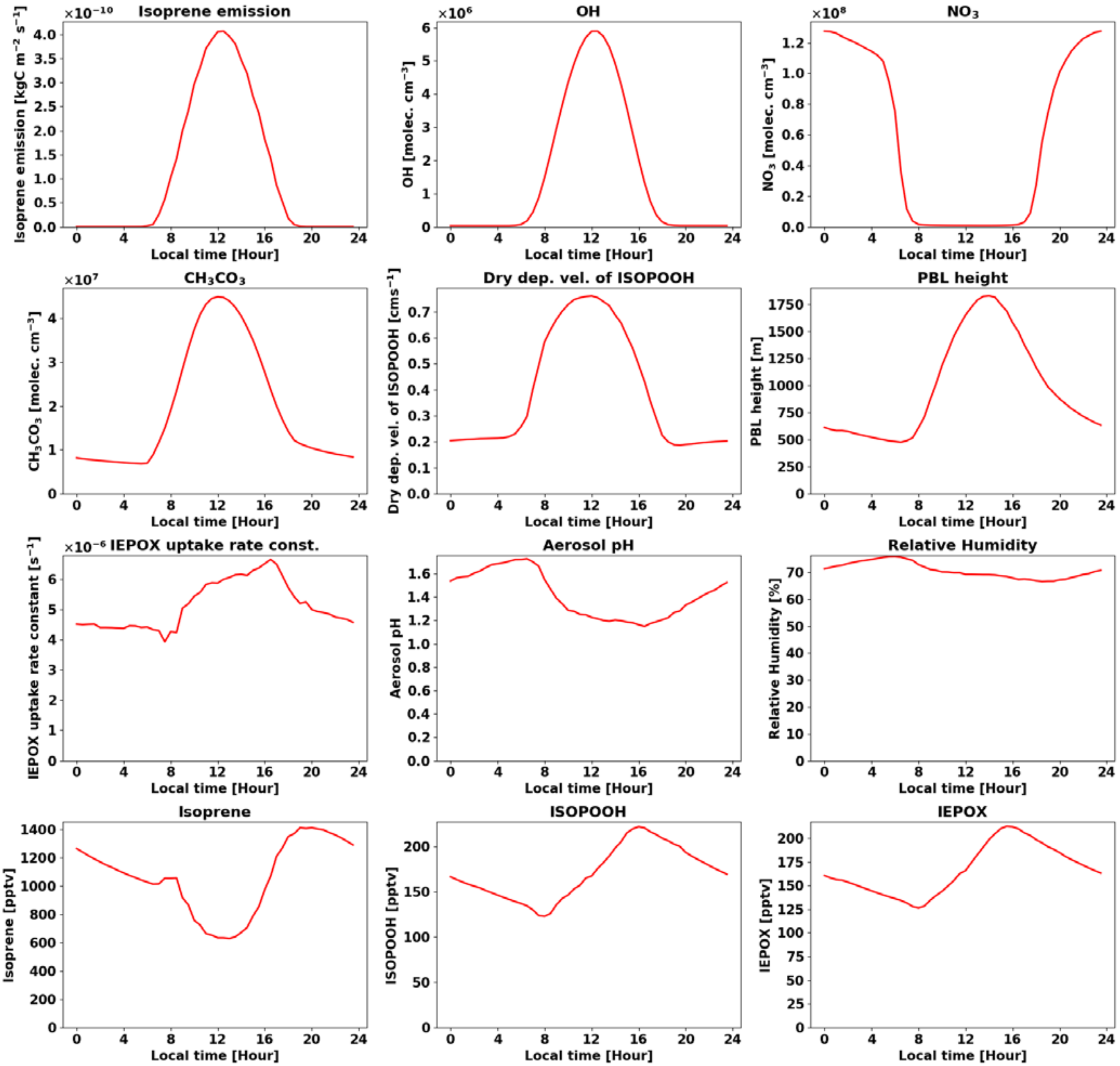

**Figure S8.** Diurnal variations of chemical/meteorological fields used in box model calculation (Fig. 5d). Values were extracted from GEOS-Chem global mean results for four major isoprene source regions [the Southeastern United States: 30°N – 40°N, 100°W – 80°W, Amazon: 10°S – 0°S, 70°W – 60°W, Central Africa: 5°N – 15°N, 10°E – 30°E, Borneo: 5°S – 5°N, 105°E – 120°E]. Figures represent approximate annual mean diurnal variation profiles, which were calculated by using the first two days of each month model outputs at 30 minutes interval averaged within the PBL, averaging points of the same local time.

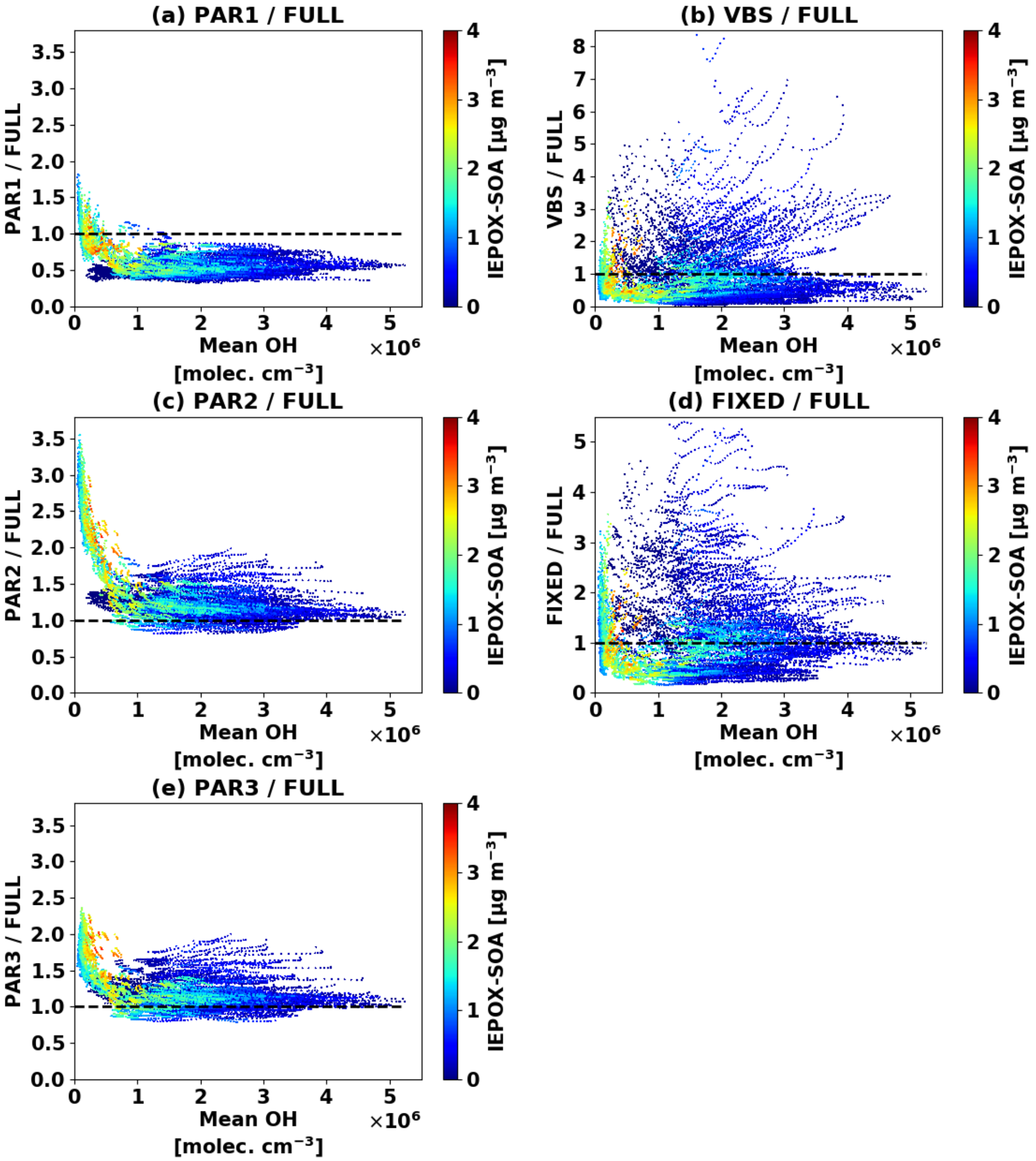

**Figure S9.** Scatterplots of the IEPOX-SOA concentration ratio (five parameterizations against the explicit full chemistry) vs. OH concentration within the PBL. Each point represents the monthly averaged model grid value for four major isoprene source regions [the Southeastern United States: 30°N – 40°N, 100°W – 80°W, Amazon: 10°S – 0°S, 70°W – 60°W, Central Africa: 5°N – 15°N, 10°E – 30°E, Borneo: 5°S – 5°N, 105°E – 120°E]. Colors indicate the IEPOX-SOA concentration simulated by the full chemistry.

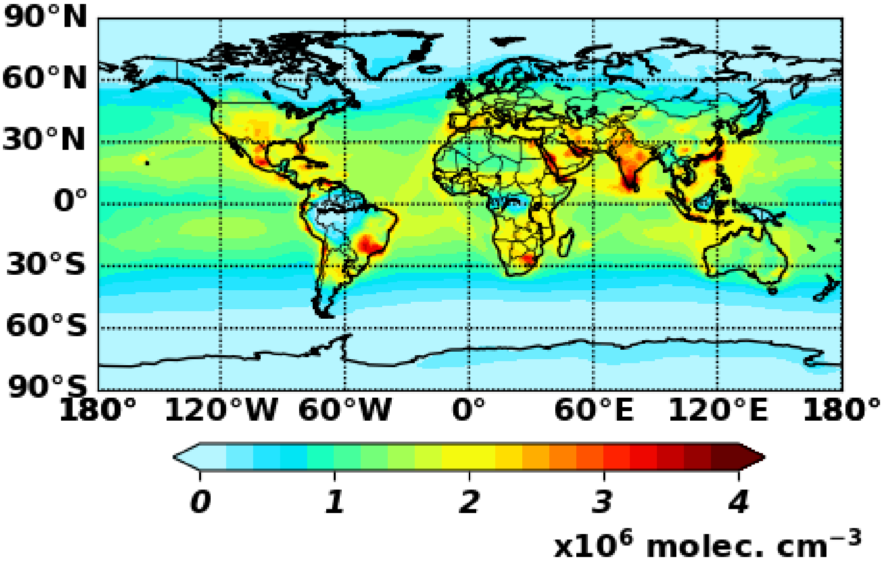

**Figure S10.** Global annual mean OH concentrations for July 2013 – June 2014 as predicted by the GEOS-Chem v11-02-rc used in this study.

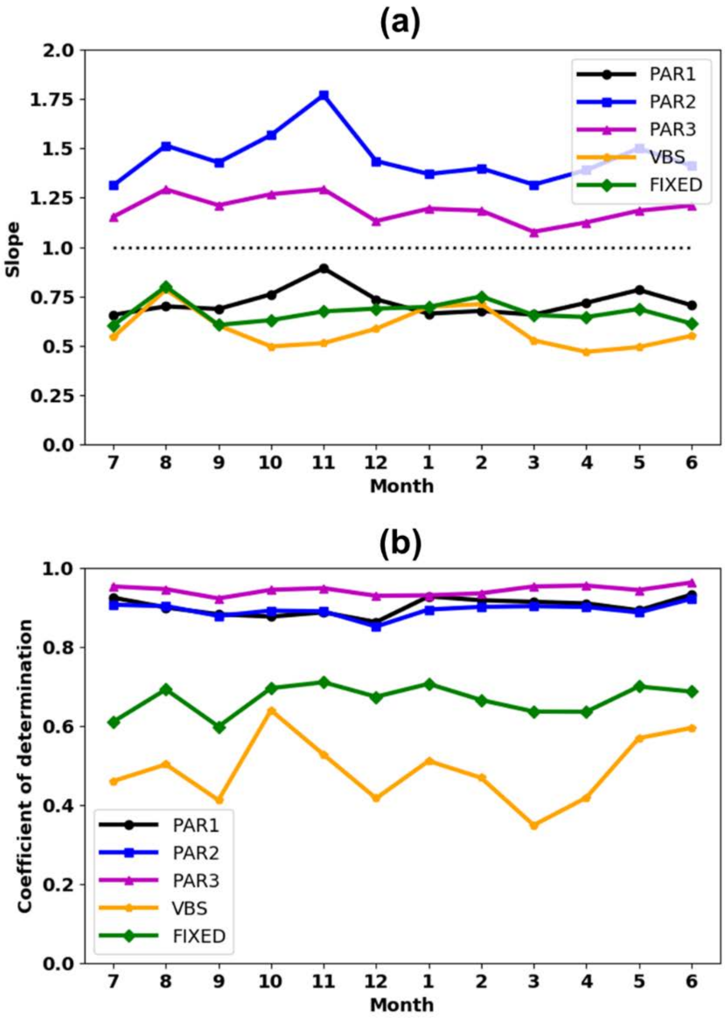

**Figure S11.** Timeseries of (a) regression slope and (b) $R^2$ for the full chemistry vs. parameterizations. Regression slope and $R^2$ are calculated for each month for concentrations within the troposphere.

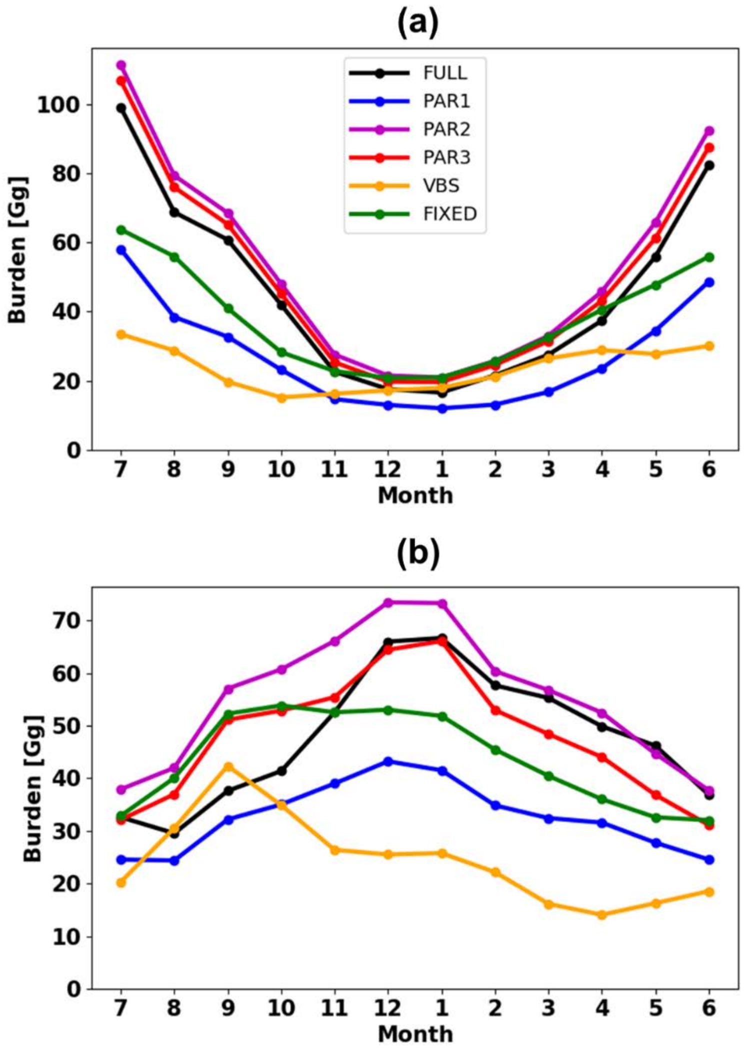

**Figure S12.** Same as Fig. 4c but for (a) Northern and (b) Southern Hemisphere.

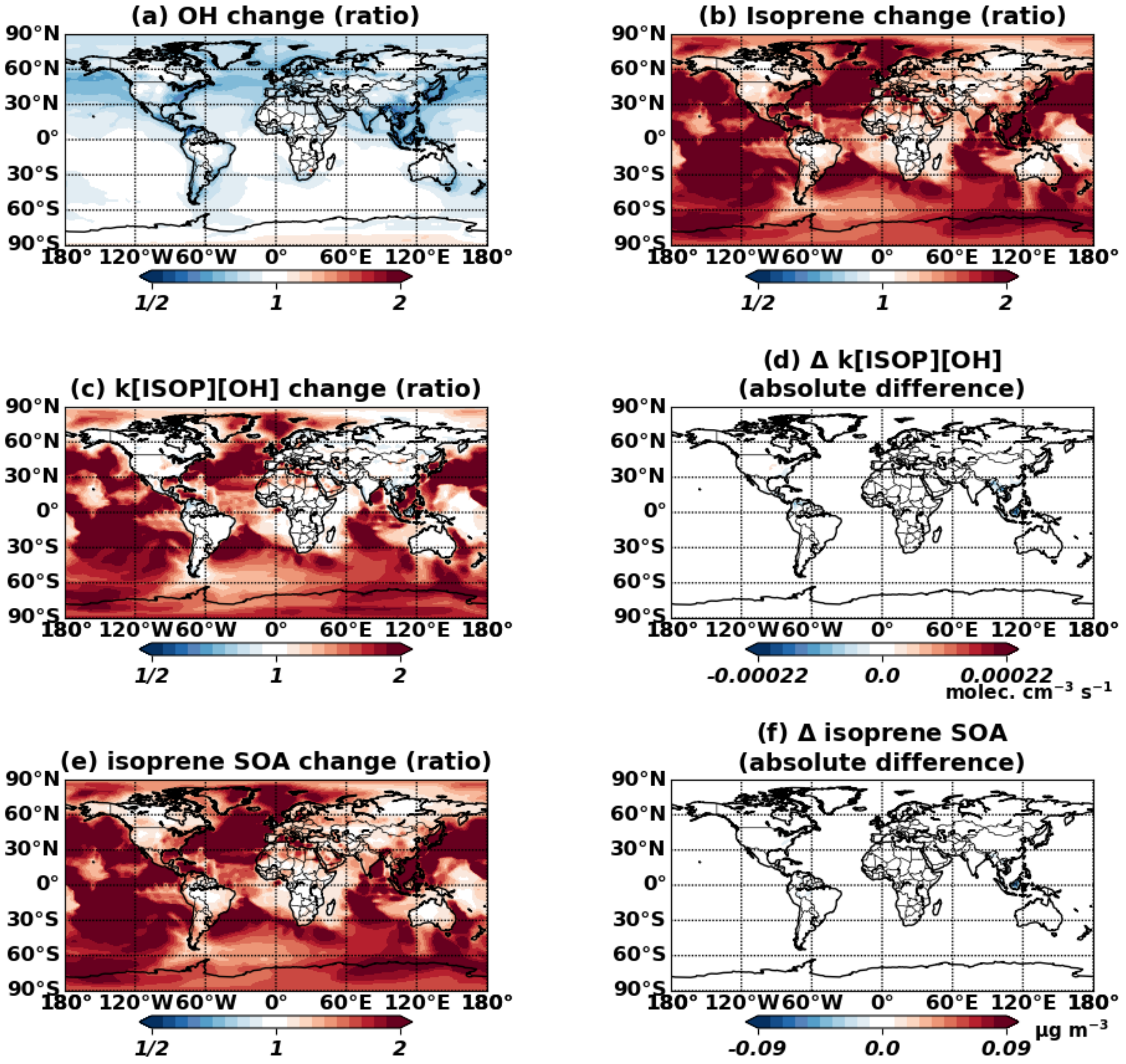

**Figure S13.** Changes of chemical fields affecting the initial oxidation of isoprene and isoprene SOA concentrations simulated by the VBS. Ratios were computed as the 50% NOx emission reduction case divided by the base case. All figures represent surface values for July – August 2013.